Double clad fibers for high-power fiber lasers

Pavel Peterka

Institute of Photonics and Electronics
The Czech Academy of Sciences
team of Fiber lasers and nonlinear optics

Europhoton 2020 Summer school, Prague, Czechia

ÚFE www.ufe.cz

First fiber lasers and amplifiers

Eli Snitzer 1960

E. Snitzer, *J. Appl. Phys.* 32(1), 36 (1961).
C. J. Koester, and E. Snitzer, *Appl. Opt.* 3(10), 1182 (1964).

Ted Maiman 1960

T. H. Maiman, Nature 187(4736), 493-494 (6 August 1960).

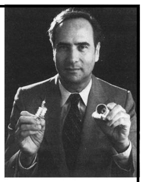

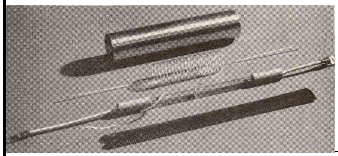

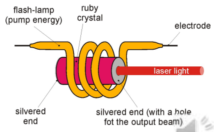

Agenda

I. Introduction 2
II. Fundamental principles, pump absorption 7
III. Limitations & LMA fibers 38
IV. Pump combiners 60
V. Technology 69
VI. Characterization 85
VII. Emerging technologies & Prospects 91

Advent of EDFA & cladding pumping for high power

Erbium doped fiber amplifier - revolution in telecom, EDFA enabled broadband internet globally.
R. J. Mears *et al.*, *Electron. Lett.* 23(19), 1026-1028 (1987).
E. Desurvire *et al.*, *Opt. Lett.* 12(11), 888-890 (1987).

High power from double-clad active fibers
ELI Snitzer, *in Proc. Opt. Fiber Sensors* (1988), p. PD5J
R. Maurer, U.S. Patent 3 808 549, (Apr. 30, 1974).
V. Gapontsev et al., ASSL (1990), p. 258-262

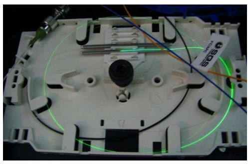

101.3 kW
Yb-fiber laser
efficiency 35.4%
IPG-Photonics
ASSL 2013

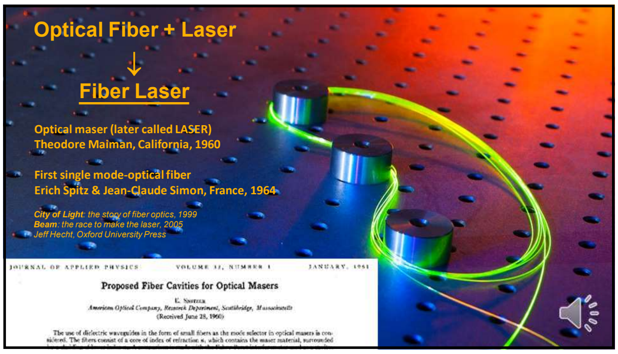

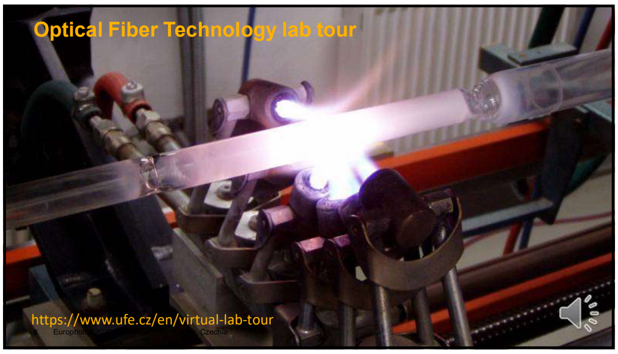

Agenda

I. Introduction 2
II. Fundamental principles, pump absorption 7
III. Limitations & LMA fibers 38
IV. Pump combiners 60
V. Technology 69
VI. Characterization 85
VII. Emerging technologies & Prospects 91

Search for optimal geometry of fiber cross section

Skew rays
Spiral trajectory projected into a polygon

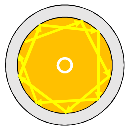

Meridional rays
Trajectory crosses the core

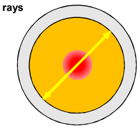

Optimal cross section provides homogenous - **constant absorption** along the DC fiber (ideal case)

Further optimization: tailoring of absorption along the DC fiber

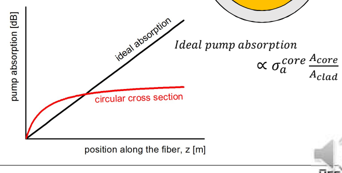

Cladding pumping – Fundamental principles

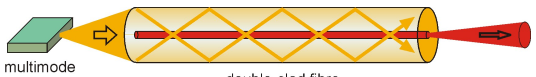

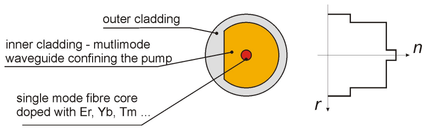

Ray optics

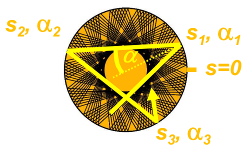

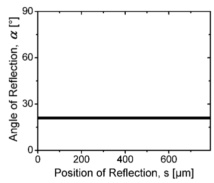

"Chaotic" ray propagation: phase diagram of s,α is filled with sufficient number of reflections.
Natural **circular shape is the worst case** of fiber cross section.

Cladding pumping – Fundamental principles

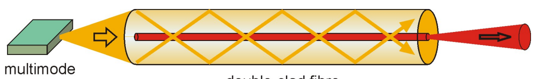

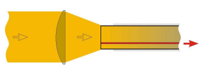

Double clad fiber – Efficient transformer of low quality beam to excellent laser beam quality

Double-clad active fibers transform a very divergent, low quality beam of high-power multimode laser diodes into a high-quality, (almost diffraction limited) laser beam

ELI Snitzer, *in Proc. OFS*(1988), p. PD5J
R. Maurer, U.S. Patent 3 808 549, (1974)
V. Gapontsev et al., ASSL (1990), p. 254-263

D-shaped fiber

Fiber thickness d > 1.5 × R

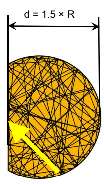

Chaotic billiard condition is confirmed

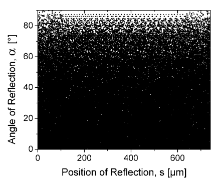

Holger Zellmer *et al*, "Doppelkern-Faserlaser," Pat. DE19535526C1, filed 1995

Valérie Doya et al., "Optimized absorption in a chaotic double-clad fiber amplifier," *Opt. Lett.* **26**, 872-874 (2001)

D-shaped fiber

Fiber thickness d < R

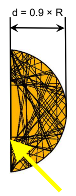

Chaotic billiard condition **is not** confirmed

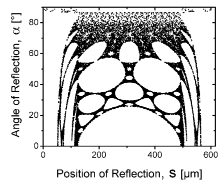

Spiral cladding

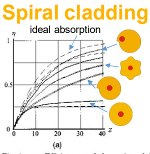

Fig. 3. (a) Efficiency η of absorption of the pump light in the core versus $Z = \mathcal{K}_0 z$. Upper dashed curve, case of ideal mixing [estimate by Eq. (9)]; dotted curve, simulation of spiral cladding with displaced core; intermediate dashed curve, the analytical estimate by formula (10); upper solid curve, numerical simulation for the same case; vertical bars, simulation for the starlike cross section; circles, simulation for spiral cladding with centered core; lowest solid curve, simulation for circular-symmetric case; lowest dashed curve, analytical estimation for the same case according to Eq. (11). (b) Efficiency of absorption of the pump light in the core of the offset-spiral double-clad fiber at $\mathcal{K}_0 = 0.005\ \mu^{-1}$, bars; $0.01\ \mu^{-1}$, dots; $0.02\ \mu^{-1}$ small circles; $0.04\ \mu^{-1}$, large circles; versus dimensionless Z.

$$\eta_{\text{ideal}} = 1 - \exp\left[-2\mathcal{K}_0\left(\frac{r_0}{R_0}\right)^2 z\right], \qquad (9)$$

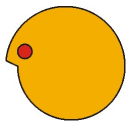

spiral cladding is made from two D-shaped preforms with different diameters

D. Kouznetsov and J. V. Moloney, "Efficiency of pump absorption in double-clad fiber amplifiers. II. Broken circular symmetry," *JOSA B* **19**, 1259-1263 (2002)

I. Dritsas, T. Sun and K. T. V. Grattan, "Stochastic optimization of conventional and holey double-clad fibres", *J. Opt. A: Pure Appl. Opt.* **9**, 405-421,2007.

N. A. Mortensen, "Air-clad fibers: pump absorption assisted by chaotic wave dynamics?," *Opt. Express* **15**(14), 8988–8996 (2007).

Most theoretical optimization of pump absorption was long time restricted to approximation of straight fibers with no bending

Experimental optimization of pump absorption by mode-scrambling

Figure eight spooling (with or without twist)

tight fiber coiling

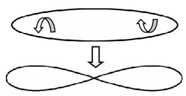

Kidney shape spooling

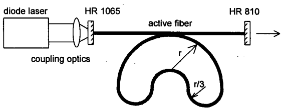

A. S. Kurkov, et al, *SPIE* **4083**, 118 (2000).
J. Nilsson et al., *IEEE J. Quantum Electronics* **39**, 987 (2003).
P. Peterka, et al., *SPIE* **6180**, 618010 (2006).
L. Shang and Z.Q.Song, *Optoel. and Adv. Mat. Rapid Comm.* **4**, 613 (2010).

H. Zellmer, *et al.*, "Double-Clad Fiber Laser with 30 W Output Power," in Proc. *Opt. Amplifiers and their Applications OAA'97*, p. FAW18 (1997).

Experiment + ray tracing and WKB modelling adopted to bending

Pump absorption in coiled double-clad fibers: numerical modelling by WKB (Wentzel-Kramers-Brillouin) method

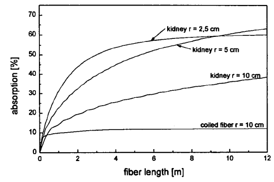

Figure 4. Pump absorption in kidney shaped fibers

Kidney shape spooling

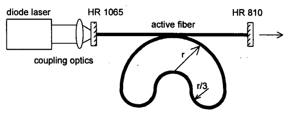

H. Zellmer, A. Tünnermann, H. Welling, and W. Reichel, "Double-Clad Fiber Laser with 30 W Output Power," in Proc. *Opt. Amplifiers and their Applications OAA'97*, Victoria, Canada, p. FAW18 (1997).

Pump absorption in coiled double-clad fibers: numerical modelling by WKB (Wentzel-Kramers-Brillouin) method

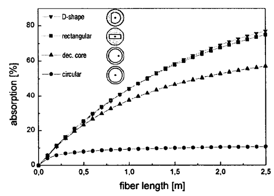

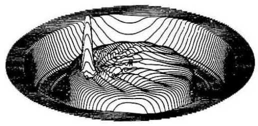

Tomography of refractive index profile of an offset-core Nd-doped fiber of the first DC fiber laser (York P101 profiler)

E. Snitzer, et al., "Double-clad, offset core Nd fiber laser," in Opt. Fiber Sensors, New Orleans, USA, 1988, pp. 533-535, paper PD5

H. Zellmer, A. Tünnermann, H. Welling, and W. Reichel, "Double-Clad Fiber Laser with 30 W Output Power," in Proc. *Opt. Amplifiers and*
their Applications OAA'97, Victoria, Canada, p. FAW18 (1997).

Model of fiber bending and twisting

Propagation of pump radiation computed using BPM (FEM and FFT based). Curvature due to coiling included using modified refractive index profile

$$n_{mod} = n_0\left(1 + \frac{x}{R}\right)$$

$$n_{mod} = n_0\left(1 + \frac{x\cos\varphi + y\sin\varphi}{R}\right)$$

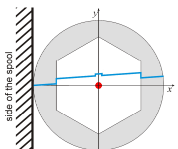

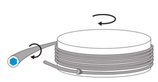

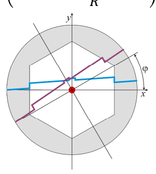

M. Heiblum & J. Harris, *IEEE J. Quantum Electron.* **11**, 75 (1975).

Pavel Koška & Pavel Peterka, Opt. Quantum Electron. 47, 318

Structures under study

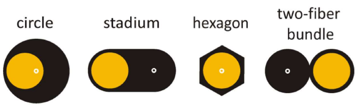

- 10 µm core diam., NA_{core}=0.17, 16 250 ppm Yb^{3+} (hexagonal fiber 3100 ppm Yb^{3+})
- Speckle beam used for excitation
- Effects of coiling, twisting, and pump injection orientation analyzed

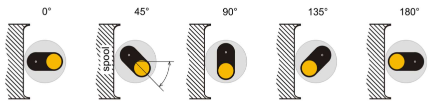

19 Europhoton 2020 Summer school, Prague, Czechia

Pump absorption in two-fiber bundle (GT-Wave)

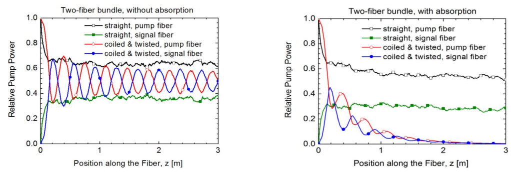

- Twisting improves the pump field coupling between fibers
- Absorption is consequently enhanced

Pavel Koška, Valérie Doya, and Pavel Peterka, *IEEE J. Sel. Top. Quantum Electron.* 22(2), 55-62 (2016).

22 Europhoton 2020 Summer school, Prague, Czechia

Pump absorption in circular fiber

Pump absorption along the circular fiber

Pump power fraction in the core of the circular fiber (pump-core overlap Γ)

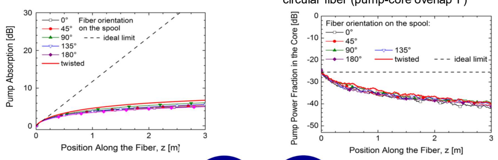

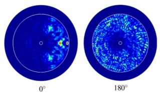

Near field orientation at the end of the spool

Pavel Koška & Pavel Peterka, Opt. Quantum Electron. 47, 3181 (2015)

20 Europhoton 2020 Summer school, Prague, Czechia

Pump absorption in hexagonal fiber

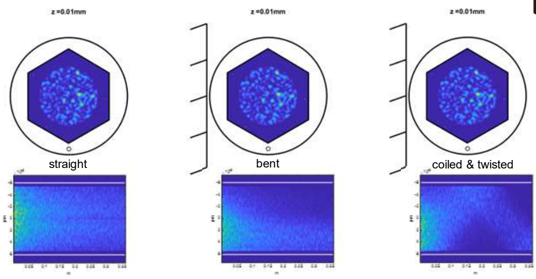

23 Europhoton 2020 Summer school, Prague, Czechia

Pump absorption in stadium-like fiber

Pump absorption along the stadium fiber

Pump power fraction in the core

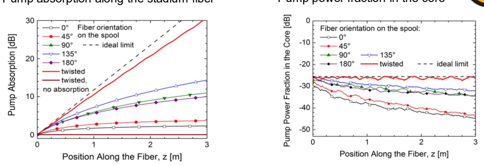

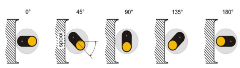

Pavel Koška & Pavel Peterka, Opt. Quantum Electron. 47, 3181 (2015)

Dependence of pump absorption on curvature radius

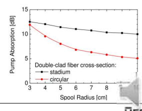

21 Europhoton 2020 Summer school, Prague, Czechia

Pump absorption: comparison among the shapes

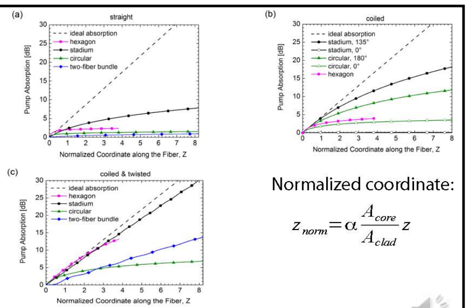

Pavel Koška, Valérie Doya, and Pavel Peterka, *IEEE J. Sel. Top. Quantum Electron.* 22(2), 55-62 (2016).

Normalized coordinate:

$$z_{norm} = \alpha \frac{A_{core}}{A_{clad}} z$$

24 Europhoton 2020 Summer school, Prague, Czechia

Pump absorption: comparison among the shapes

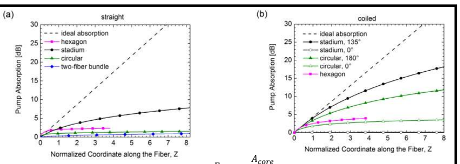

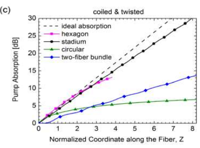

$$\Gamma_{ideal} = \frac{A_{core}}{A_{clad}}$$

Pump power fraction in the core (overlap factor Γ)

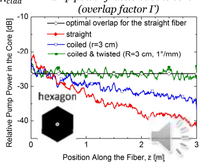

Pavel Koška, Valérie Doya, and Pavel Peterka, *IEEE J. Sel. Top. Quantum Electron.* 22(2), 55-62 (2016).

Spiral coiling

*Cladding shapes: **Superformula** of natural and abstract shapes, **Am. J. of Botany**, 90:333 (2003).*

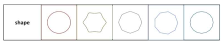

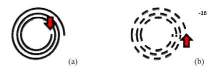

Figure 4. a) pumping from the inner of the spiral, b) pumping from the outer of the spiral

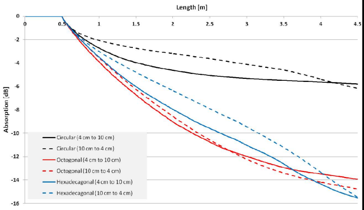

Ch. A. Codemard, A. Malinowski, and M. N. Zervas, "Numerical optimisation of pump absorption in doped double-clad fiber with transverse and longitudinal perturbation," Proc. SPIE 10083, p. 1008315 **Photonics West 2017**

Experimental verification of enhanced pump absorption

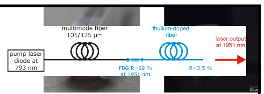

Difference of the pump absorption between the simultaneously coiled and twisted fiber and coiled only fiber for 3 m long hexagonal fiber.

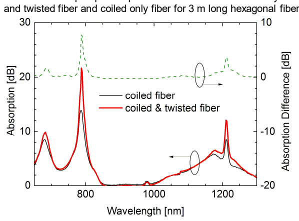

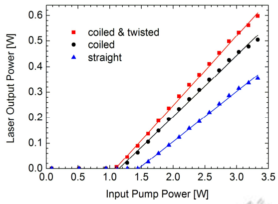

Pavel Koška, et al, *Opt. Express*, 24(1):102 (2016).

Slope Efficiency: 19.6 < 24 < 29.4 %, **50 % increase of SE**

Modal Spectra Analysis

$$E_r(x,y) = \sum_n B_n\, u_n(x,y)$$

$$E(x,y,z) = \sum_m A_m\, u_m(x,y)e^{-i\beta_m z}$$

$$P(z) = \int E_r^*(x,y)\, E(x,y,z)\mathrm{d}\Omega$$

$$\Im\{P\}_{(\beta)} = \sum_m B_m^*\, A_m \delta(\beta - \beta_m)$$

Reference field

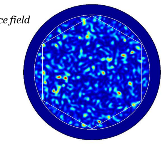

Fundamental mode field

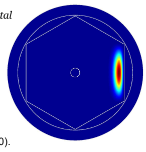

M. D. Feit and J. A. Fleck, "Computation of mode properties in optical fiber waveguides by a propagating beam method," *Applied Optics* 19(7), 1154-1164 (1980).

Twisted Tm-doped fiber with twist frozen during drawing

Tm^{3+} is ~11000 mol ppm (3 wt%) 2.24 rotations per meter (0.8°/mm), which was increased to 4.55 rotations per meter (1.6°/mm).

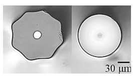

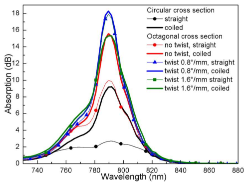

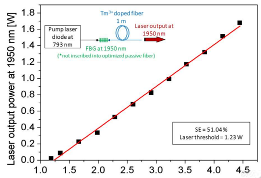

A. A. Jasim, J. Aubrecht, P. Peterka, et al., CLEO/Europe-EQEC, Munich, Germany, pp. CJ-P.8 (2019).

Modal spectra evolution in passive hexagonal fiber

Coiled fiber

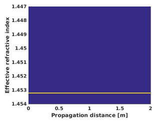

Coiled & twisted fiber

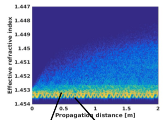

Initial fundamental mode field

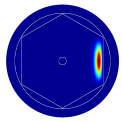

'Edge' mode *'Corner' mode*

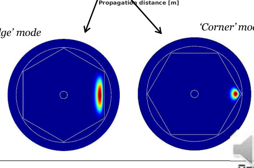

P. Koška, V. Doya, and P. Peterka, in *SPIE Photonics West: Fiber Lasers XIV*, San Francisco, USA, 2017, p. 100830U.

Modal spectra evolution in hexagonal vs. circular fiber

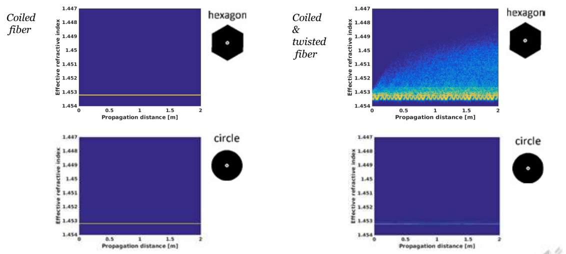

P. Koška, V. Doya, and P. Peterka, in *SPIE Photonics West: Fiber Lasers XIV*, San Francisco, USA, 2017, p. 10083

Pump modal spectra evolution in active hexagonal fiber

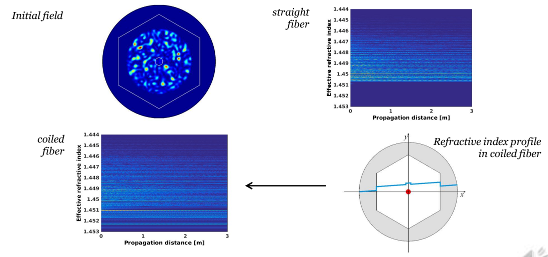

P. Koška, V. Doya, and P. Peterka, in *SPIE Photonics West: Fiber Lasers XIV*, San Francisco, USA, 2017, p. 10083

Pump modal spectra evolution: speckle pattern case

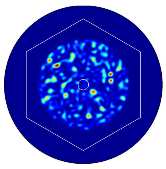

Initial field

Parameters of Yb doped active hexagonal fiber

Core diameter	12 µm
Cladding diameter (flat to flat)	130 µm
Core refractive index	1.4556
Cladding refractive index	1.4507
Coating refractive index	1.4027
Yb Concentration	4.54 x 10^{25} m^{-3} (2200 mol ppm Yb^{3+})
Pump wavelength	975 nm
Signal wavelength	1020 nm

P. Koška, V. Doya, and P. Peterka, in *SPIE Photonics West: Fiber Lasers XIV*, San Francisco, USA, 2017, p. 10083

Pump modal spectra evolution in active hexagonal fiber

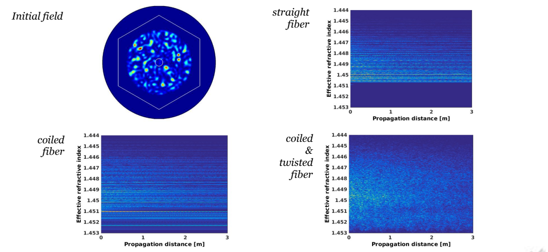

P. Koška, V. Doya, and P. Peterka, in *SPIE Photonics West: Fiber Lasers XIV*, San Francisco, USA, 2017, p. 10083

Pump modal spectra evolution in active hexagonal fiber

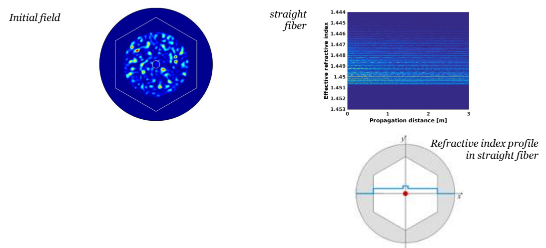

P. Koška, V. Doya, and P. Peterka, in *SPIE Photonics West: Fiber Lasers XIV*, San Francisco, USA, 2017, p. 10083

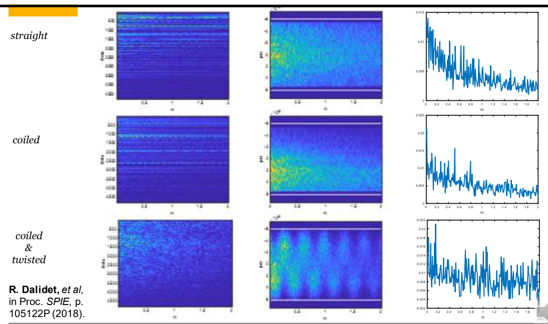

R. Dalidet, *et al*, in Proc. *SPIE*, p. 105122P (2018).

Pump absorption in DC fibers: things to remember

- **Pump absorption is enhanced** by **broken circular symmetry** of inner cladding cross section and by **unconventional coiling methods**

But remember: non-circular fiber shapes do not help for mode mixing in strictly straight fibers and bent-only fibers; do not forget on **pump squeezing** and **decentering effects.**

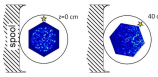

- **Approximation of cladding pump absorption:** $\propto \sigma_a^{core} \frac{A_{core}}{A_{clad}}$

$\Gamma_{ideal} = \frac{A_{core}}{A_{clad}}$

It is often used in numerical modelling and quick design of fiber lasers but use it wisely. **It is only approximation!**

In fact the true is the opposite, that overlap factor Γ is never constant along the fiber, for some geometry it can gets close to the ideal case.

Pump power fraction in the core (overlap factor Γ)

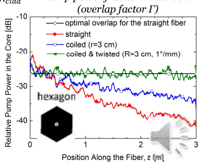

Pavel Koška, Valérie Doya, Pavel Peterka, *IEEE J. Sel. Top. Quantum Electron.* **22**, 55 (2016).
Pavel Koška, *et al*, *Opt. Express* **24**, 102-107 (2016).

Tandem pumped Yb fiber laser pumped at 1018 nm

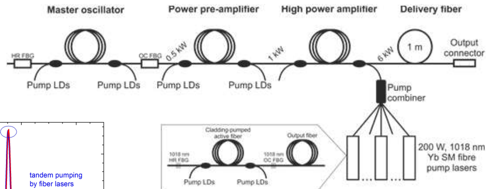

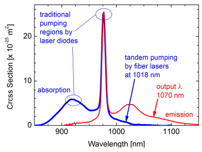

according to IPG Photonics presentation at SPIE Photonics West

Agenda

I. Introduction 2
II. Fundamental principles, pump absorption 7
III. Limitations & LMA fibers 38
IV. Pump combiners 60
V. Technology 69
VI. Characterization 85
VII. Emerging technologies & Prospects 91

Power scaling limits due to nonlinear effects

Stimulated Brillouin Scattering (SBS) $P_{SBS} = 21\frac{A_{eff}}{g_B L_{eff}}$ $g_B = 3-5\times10^{-11}\,\frac{\mathrm{m}}{\mathrm{W}}$

Stimulated Raman Scattering (SRS) $P_{SRS} = 16\frac{A_{eff}}{g_R L_{eff}}$ $g_R = 0.5\times10^{-13}\,\mathrm{m/W}$

Raman scattering: 13 THz (44nm @1000 nm, 92nm @1460 nm) Brillouin s.: 10 GHz (backward)

Self focusing $P_{SF} = \frac{0.148\,\lambda^2}{n_0 n_2}$ $n_2 = 2.2\times10^{-20}\,\frac{\mathrm{m}^2}{W}$

Self-phase modulation $P_{SF} \cong 5.2$ MW at 1 μm, >20 MW at 2 μm

Rudiger Paschotta, RP Photonics Encyclopedia, https://www.rp-photonics.com/encyclopedia.html
Arlee V. Smith *et al*, "Optical damage limits to pulse energy from fibers," *IEEE J. Sel. Top. Quantum Electron.* **15**, 153-158 (2009).
L. Dong, B. Samson, Fiber Lasers: Basics, Technology, and Applications, Boca Raton, CRC Press 2016.

DC fiber limits & Power scaling

Single-mode, diode pumped (SM-DP) fiber lasers

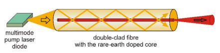

Single-mode, tandem pumped (SM-TP) fiber lasers

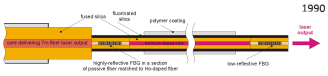

Rise of power of Yb-doped fiber lasers

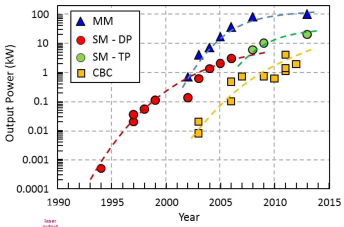

M. N. Zervas, C. A. Codemard, "High power fiber lasers: a review," *IEEE J. Sel. Topics Quantum Electron.* **20**, 0904123 (2014).

Nonlinearity issue remedy: Large Mode Area (LMA) fibers

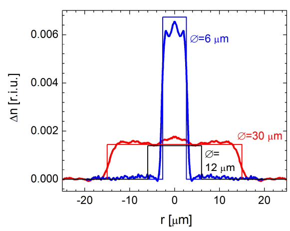

Corning HI1060, NA=0.14, λ=1.06 μm

$\varnothing_{core}$	V	MFD	A_{eff}	Number of modes
5.3 μm	2.20	6.2 μm	30 μm²	1

LMA fibers with various $\varnothing_{core}$, NA=0.06, λ=1.06 μm

$\varnothing_{core}$	V	MFD	A_{eff}	Number of modes
12 μm	2.13	14.4 μm	163 μm²	1
15 μm	2.67	15.4 μm	187 μm²	2
20 μm	3.55	17.9 μm	250 μm²	2
30 μm	5.33	23.4 μm	432 μm²	4

Higher-Order Mode (HOM) filtering by coiling

Coil geometry matters: the invention of large mode area (LMA) fibres and methods to maintain single mode operation of LMA fibres is one of major breakthroughs in power scaling of fiber lasers.

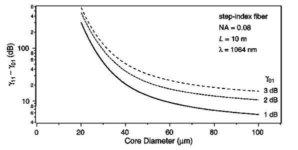

Fig. 1. Calculated values of the LP_{11} suppression relative to LP_{01} versus core diameter at the indicated values of γ_{01}. The choice of $L = 10$ m is representative; for other fiber lengths, similar levels of LP_{11} suppression are calculated for a given γ_{01} at slightly different values of D.

J. P. Koplow, D. A. V. Kliner, L. Goldberg, *Opt. Lett.* **25**, 442 (2000).

Other methods of SM regime of few mode core:
- tapering of the few-mode fiber
- LP01 mode gain preference by confined doping
- Multi-trench fiber design
- Chirally coupled core
- Twisted fiber with broken circular symmetry of the core
- resonant filtering by leakage channel fiber or all-solid PBG fiber
- and others

Most widely used and experimentally simple is still the HOM filtering by coiling

Squeezing A_{eff} of LMA fibers due to coiling

Coil geometry matters: tight coiling reduces Aeff, namely in larger core LMA fibers

Joel M. Fini, "Bend-resistant design of conventional and microstructure fibers with very large mode area," *Opt. Express* **14**, 69-81 (2006).

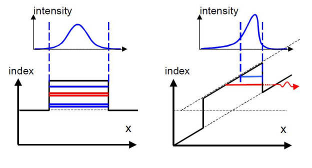

Fig. 4. The equivalent-index model gives us an intuitive picture of bend-induced distortion and area reduction. Bends lead to an index gradient across the core, which tends to push light towards the outside of the bend. The index plot includes the fiber index profile (black) and effective index of the modes (red and blue).

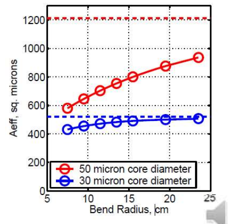

Squeezing A_{eff} of LMA fibers due to coiling

Coil geometry matters: tight coiling reduces Aeff, namely in larger core LMA fibers

Joel M. Fini, "Bend-resistant design of conventional and microstructure fibers with very large mode area," *Opt. Express* **14**, 69-81 (2006).

core diameter:

30 µm

50 µm

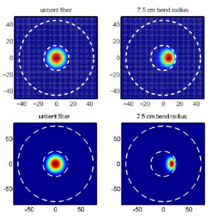

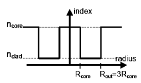

Fig. 2. This W-shaped index profile was used for the two fibers of Fig. 1. For both fibers, the outer cladding has the same index as the core, and $R_{out} = 3R_{core}$.

Squeezing A_{eff} of LMA fibers due to coiling

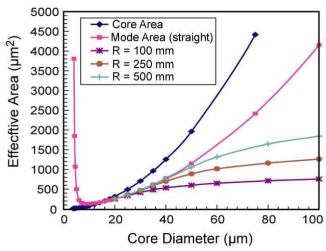

Plot of effective mode area as a function for core diameter for varying bend radii. Core NA=0.06 in all cases.

Jay W. Dawson, et al., "Analysis of the scalability of diffraction-limited fiber lasers and amplifiers to high average power," *Opt. Express* **16**(17), 13240 (2008).

Squeezing A_{eff} of LMA fibers due to coiling

Coil geometry matters: tight coiling reduces Aeff, namely in larger core LMA fibers

Joel M. Fini, "Bend-resistant design of conventional and microstructure fibers with very large mode area," *Opt. Express* **14**, 69-81 (2006).

core diameter:

30 µm

50 µm

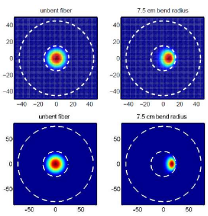

Do you remember mode-area squeezing in inner cladding of DC fiber? Despite much larger core size, the effect is also important:

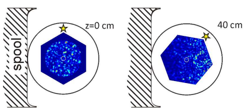

P. Koska, P. Peterka, J. Aubrecht, *et al*, "Enhanced pump absorption efficiency in coiled and twisted double-clad thulium-doped fibers," *Opt. Express* **24**, 102-107 (2016).

Rod-type LMA fibers

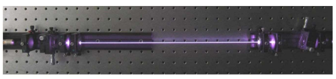

Jens Limpert, *et al.*, "High-power rod-type photonic crystal fiber laser," *Opt. Express* **13**(4), 1055-1058 (2005).

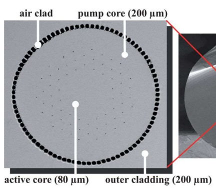

A. Tünnermann, T. Schreiber, and J. Limpert, "Fiber lasers and amplifiers: an ultrafast performance evolution," *Appl. Optics* **49**, F71-F78 (2010).

corner-to-corner 80 µm
inner cladding: 200 µm, → high pump overlap → clad. abs. 30 dB/m
A_{eff} ~ 4000 µm².
$NA_{air\text{-}clad}$ as high as 0.6

Fiber heating

Analytical formula for estimation of surface temperature between the silica innercladding and the fluorinated polymer:

core: $T_1(r) = T_{a1} - \frac{P_{heat}\, r^2}{4k_1}$

cladding layers: $T_3(r) = T_b + \frac{P_{heat}\, a_1^2}{2k_3}\left(\ln\frac{r}{a_2} + \ln\frac{a_3}{a_2}\right)$

power density of the heat source P_{heat} [W/m³]

and $T_3(a_2) = T_b + \frac{P_{heat,L}}{2\pi k_3}\ln\frac{a_3}{a_2}$

for the power density of the heat source $P_{heat,L}$ [W/m]

thermal conductivities, *k[W/mK]*: silica 1.38, acrylate 0.18, aluminium 238

Fiber geometry with two claddings, i. e., three surfaces N=3, T_b is the background (boundary) temperature

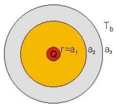

Temperature at the boundary between silica inner cladding and polymer outer cladding – the weak point of the double clad fiber

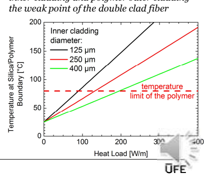

Similar analysis is given in:
D. C. Brown and H. J. Hoffman, "Thermal, stress, and thermo-optic effects in high average power double-clad silica fiber lasers," *IEEE J. Quantum Electron.* **37**, 207-217 (2001).

Fiber heating in circular DC fiber: analytical formula vs. FEM

Graphs by Martin Grábner
Wednesday 2nd Sept. 19:30
„Numerical study of effect of bending and twist on pump absorption in octagonal double-clad fiber"

Temperature distribution calculated by analytical formula and FEM modelling (COMSOL Multiphysics):

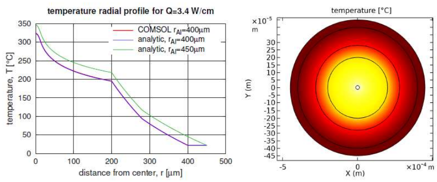

Temperature distribution of the circular fiber sitting in an aluminium tube

Fiber heating in 10/130 Tm fiber

Temperature distribution calculated by FEM modelling (COMSOL Multiphysics):

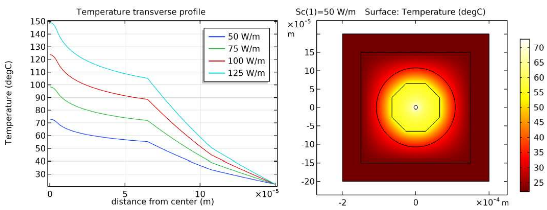

Temperature distribution of the 10/130 µm octagonal fiber sitting in the grooves in the cooling plate

Fiber heating in 20/250 Tm fiber

Temperature distribution calculated by FEM modelling (COMSOL Multiphysics):

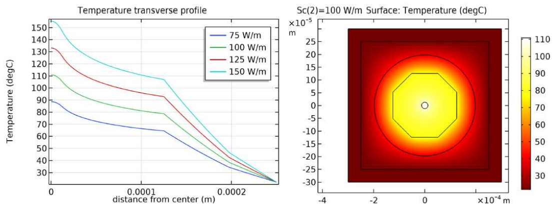

Temperature distribution of the 20/250 µm octagonal fiber sitting in the grooves in the cooling plate

Fiber heating in 25 µm core, air-clad fiber

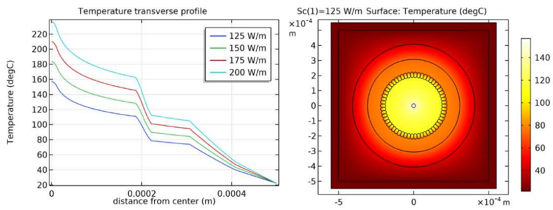

Heat load varies along the fiber, even with 1150 W average power Tm fiber it is estimated to be below 200 W/m, on average 98 W/m in 50/250 TmPCF.

C. Gaida, M. Gebhardt, T. Heuermann, F. Stutzki, C. Jauregui, and J. Limpert, "Ultrafast thulium fiber laser system emitting more than 1 kW of average power," *Opt. Lett.* **43**(23), 5853-5856 (2018).

Thermal lensing & Transverse mode instability

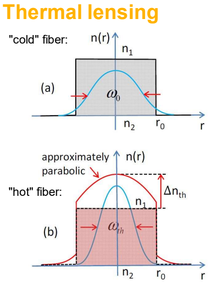

M. N. Zervas, *Opt. Express* **27**, 19019 (2019).

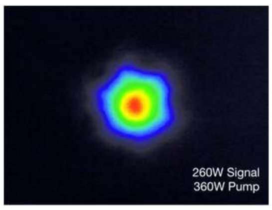

Source of the video: T. Eidam, C. Wirth, C. Jauregui, F. Stutzki, F. Jansen, H. Otto, O. Schmidt, T. Schreiber, J. Limpert, and A. Tünnermann, "Experimental observations of the threshold-like onset of mode instabilities in high power fiber amplifiers," *Opt. Express* **19**, 13218 (2011).
©OSA, CC license, link: https://doi.org/10.1364/OE.19.013218

Transverse mode instability

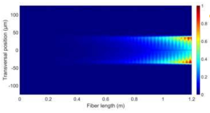

C. Jauregui *et al*, *Opt. Express* **24**, 7879 (2016).

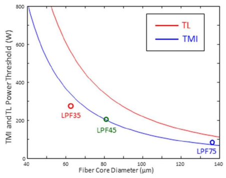

M. N. Zervas, *Opt. Express* **27**, 19019 (2019).

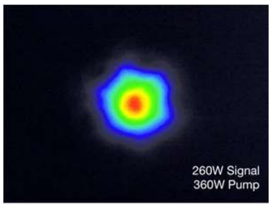

Source of the video: T. Eidam, C. Wirth, C. Jauregui, F. Stutzki, F. Jansen, H. Otto, O. Schmidt, T. Schreiber, J. Limpert, and A. Tünnermann, "Experimental observations of the threshold-like onset of mode instabilities in high power fiber amplifiers," *Opt. Express* **19**, 13218 (2011).

©OSA, CC license, link: https://doi.org/10.1364/OE.19.013218

Longitudinal mode instability

Laser λ self-sweeping - special case of **longitudinal mode instability**

Kir'yanov, Il'ichev, *Laser Phys. Lett* **8**, 305 (2011).
Lobach *et al*, *Opt. Express* **19**(18), 17632 (2011).
Peterka et al, *Laser Phys. Lett.* **6**, 732 (2009), and *Laser Phys. Lett.* 9, 445 (2012).

$$\Delta\nu = \frac{c}{2nL}, \Delta\lambda = \frac{\lambda^2 \Delta\nu}{c}$$

L=10 m, Δν=10 MHz
10 nm gain bw.→
3×10^5 modes

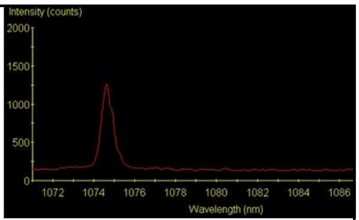

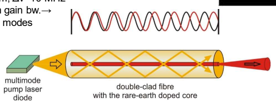

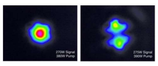

T. Eidam et al, Optics Express 19, 13218 (2011).

Longitudinal mode instability

Laser λ self-sweeping - special case of **longitudinal mode instability**

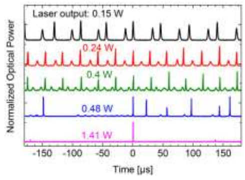

P. Peterka, *et al.*, *Opt. Express* **22**, 30024 (2014).

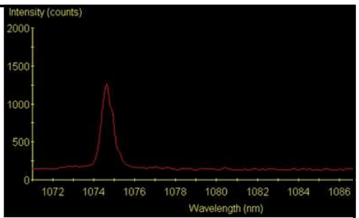

Tips for further readings:

- P. Peterka, P. Koška, and J. Čtyroký, "Reflectivity of superimposed Bragg gratings induced by longitudinal mode instabilities in fiber lasers," *IEEE J. Sel. Topics Quantum Electron.* **24**, 0902608 (2018).
- I. A. Lobach, S. I. Kablukov, E. V. Podivilov, and S. A. Babin, "Self-scanned single-frequency operation of a fiber laser driven by a self-induced phase grating," *Laser Phys. Lett.* **11**, 045103 (2014).

Challenges specific to rare earth ions

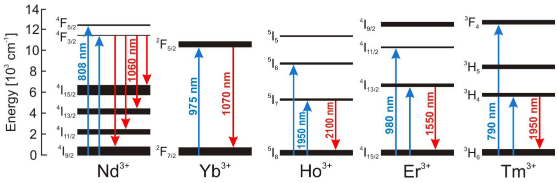

Photodarkening

- Permanent, light-induced **increase of absorption** of the fiber (mainly in visible range)
- Multiphoton process involving rare-earth ion (observed in ytterbium, thulium ...)
- It is caused by the **formation of color centers**, formed by photoionization
- RE ion gets energy directly by photon absorption or by migration processes
- **High inversion of population increases photodarkening rate** → photodarkening is slow in continuous-wave DC fiber lasers but fast in amplifiers, broadband ASE (Amplified Spontaneous Emission) sources and core-pumped fiber laser devices
- mitigation by material composition and device configuration (lower inversion)

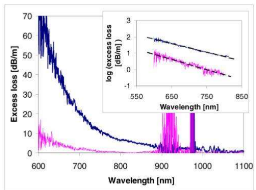

Joona Koponen, *et al.*, *Opt. Express* **14**, 11539 (2006)

Agenda

I. Introduction 2
II. Fundamental principles, pump absorption 7
III. Limitations & LMA fibers 38
IV. Pump combiners 60
V. Technology 69
VI. Characterization 85
VII. Emerging technologies & Prospects 91

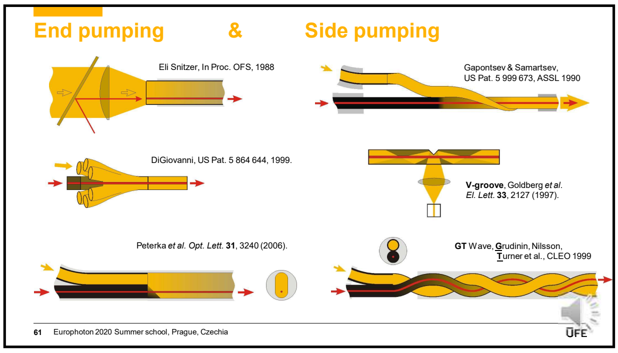
End pumping & Side pumping
Eli Snitzer, In Proc. OFS, 1988
Gapontsev & Samartsev, US Pat. 5 999 673, ASSL 1990
DiGiovanni, US Pat. 5 864 644, 1999.
V-groove, Goldberg et al. El. Lett. 33, 2127 (1997).
Peterka et al. Opt. Lett. 31, 3240 (2006).
GT Wave, Grudinin, Nilsson, Turner et al., CLEO 1999
61 Europhoton 2020 Summer school, Prague, Czechia
ÚFE

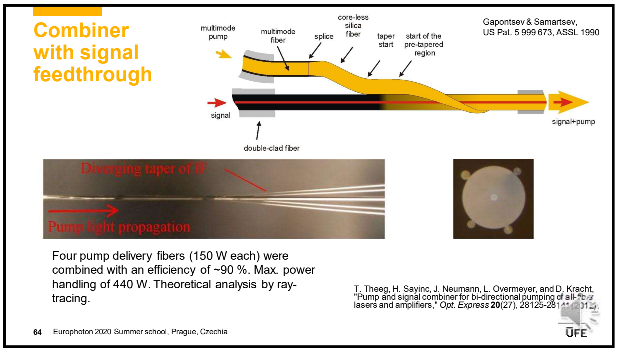
Combiner with signal feedthrough
multimode pump
multimode fiber
splice
core-less silica fiber
taper start
start of the pre-tapered region
Gapontsev & Samartsev, US Pat. 5 999 673, ASSL 1990
signal
double-clad fiber
signal+pump
Diverging taper of H
Pump light propagation
Four pump delivery fibers (150 W each) were combined with an efficiency of ~90 %. Max. power handling of 440 W. Theoretical analysis by ray-tracing.
T. Theeg, H. Sayinc, J. Neumann, L. Overmeyer, and D. Kracht, "Pump and signal combiner for bi-directional pumping of all-fiber lasers and amplifiers," Opt. Express 20(27), 28125-281
64 Europhoton 2020 Summer school, Prague, Czechia
ÚFE

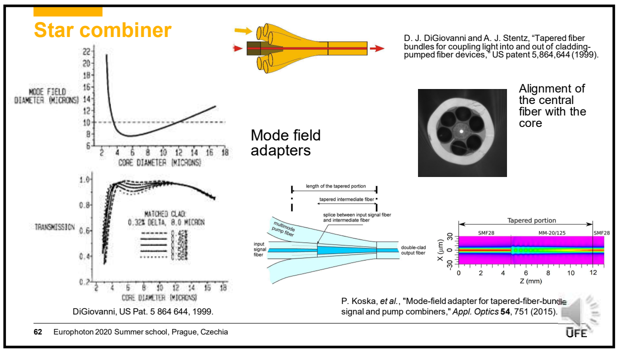
Star combiner
D. J. DiGiovanni and A. J. Stentz, "Tapered fiber bundles for coupling light into and out of cladding-pumped fiber devices," US patent 5,864,644 (1999).
MODE FIELD DIAMETER (MICRONS)
CORE DIAMETER (MICRONS)
TRANSMISSION
MATCHED CLAD: 0.32% DELTA, 8.0 MICRON
Mode field adapters
Alignment of the central fiber with the core
Tapered portion
X (μm)
Z (mm)
DiGiovanni, US Pat. 5 864 644, 1999.
P. Koska, et al., "Mode-field adapter for tapered-fiber-bundle signal and pump combiners," Appl. Optics 54, 751 (2015).
62 Europhoton 2020 Summer school, Prague, Czechia
ÚFE

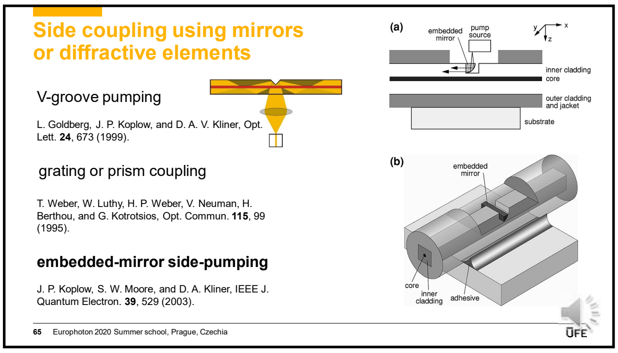
Side coupling using mirrors or diffractive elements
V-groove pumping
L. Goldberg, J. P. Koplow, and D. A. V. Kliner, Opt. Lett. 24, 673 (1999).
grating or prism coupling
T. Weber, W. Luthy, H. P. Weber, V. Neuman, H. Berthou, and G. Kotrotsios, Opt. Commun. 115, 99 (1995).
embedded-mirror side-pumping
J. P. Koplow, S. W. Moore, and D. A. Kliner, IEEE J. Quantum Electron. 39, 529 (2003).
(a)
embedded mirror
pump source
inner cladding
core
outer cladding and jacket
substrate
(b)
embedded mirror
core
inner cladding
adhesive
65 Europhoton 2020 Summer school, Prague, Czechia
ÚFE

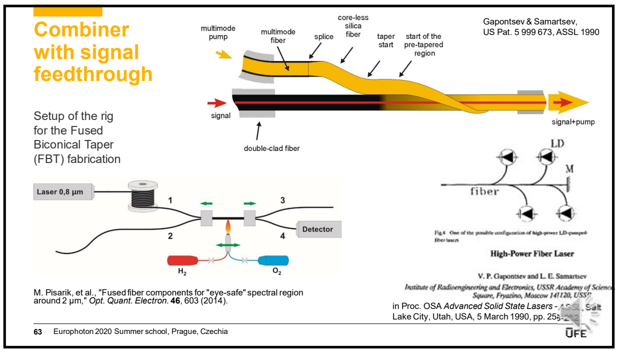
Combiner with signal feedthrough
multimode pump
multimode fiber
splice
core-less silica fiber
taper start
start of the pre-tapered region
Gapontsev & Samartsev, US Pat. 5 999 673, ASSL 1990
signal
double-clad fiber
signal+pump
Setup of the rig for the Fused Biconical Taper (FBT) fabrication
Laser 0,8 μm
Detector
fiber
High-Power Fiber Laser
V. P. Gapontsev and L. E. Samartsev
M. Pisarik, et al., "Fused fiber components for "eye-safe" spectral region around 2 μm," Opt. Quant. Electron. 46, 603 (2014).
in Proc. OSA Advanced Solid State Lasers - Salt Lake City, Utah, USA, 5 March 1990, pp. 25
63 Europhoton 2020 Summer school, Prague, Czechia
ÚFE

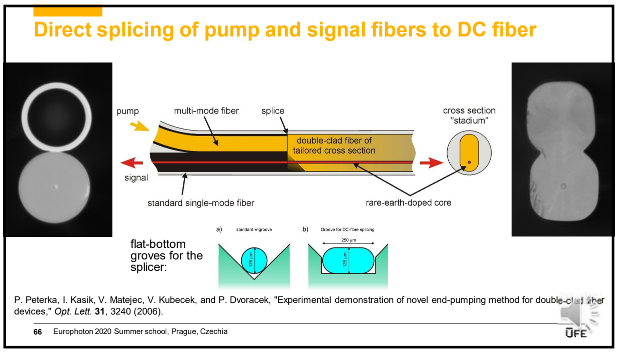
Direct splicing of pump and signal fibers to DC fiber
pump
multi-mode fiber
splice
cross section "stadium"
double-clad fiber of tailored cross section
signal
standard single-mode fiber
rare-earth-doped core
flat-bottom groves for the splicer:
P. Peterka, I. Kasik, V. Matejec, V. Kubecek, and P. Dvoracek, "Experimental demonstration of novel end-pumping method for double-clad fiber devices," Opt. Lett. 31, 3240 (2006).
66 Europhoton 2020 Summer school, Prague, Czechia
ÚFE

Double clad fiber bundle structure

GT Wave

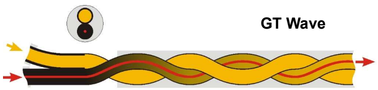

Anatoly B. Grudinin, et al., "**Multi-fibre** arrangements for high power fiber lasers and amplifiers," US Pat. 6 826 335, 2004.

Grudinin, Nilsson, Turner et al., CLEO 1999

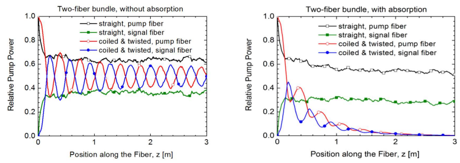

Fiber twist matters

Pavel Koška, Valérie Doya, and Pavel Peterka, *IEEE J. Sel. Top. Quantum Electron.* **22**, 55-62 (2016).

Double clad fiber bundle structure

GT Wave

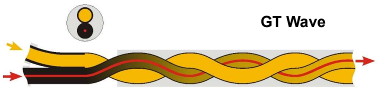

Anatoly B. Grudinin, et al., "**Multi-fibre** arrangements for high power fiber lasers and amplifiers," US Pat. 6 826 335, 2004.

Grudinin, Nilsson, Turner et al., CLEO 1999

Short fiber amplifying modules (~10 cm) using RE-doped **phosphate** glass fibers

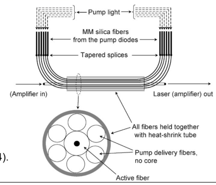

P. Polynkin, *et al.*, "Efficient and scalable side pumping scheme for short high-power optical fiber lasers and amplifiers," *IEEE Photon. Technol. Lett.* **16**, 2024 (2004).

Agenda

I.	Introduction	2
II.	Fundamental principles, pump absorption	7
III.	Limitations & LMA fibers	38
IV.	Pump combiners	60
V.	Technology	69
VI.	Characterization	85
VII.	Emerging technologies & Prospects	91

Optical Fiber Technology

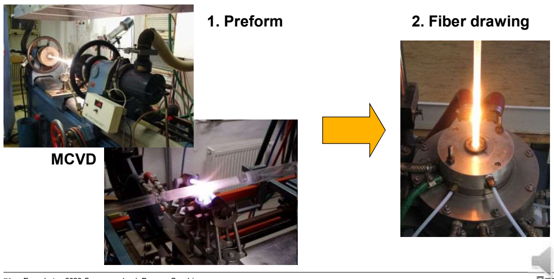

MCVD – Modified Chemical Vapor Deposition and solution doping methods

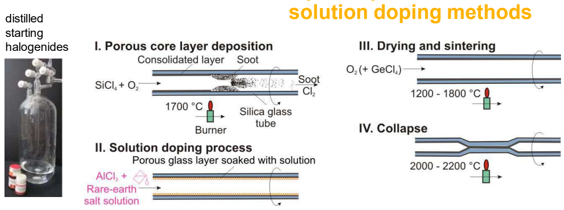

Other methods: Plasma Chemical Vapor deposition (PCVD), Outside Vapor Deposition, Chelate delivery, hybrid gas-phase solution doping, direct nanoparticle deposition (DND by Liekki/nLight), sol-gel methods, sintered powder methods (REPUSIL) etc.

Nanoparticle & solution doping methods

Two ways were proposed in the original paper (2007) about the nanoparticle dispersion:

1. Alumina nanoparticles + RE chlorides
2. Synthesized alumina nanoparticles already containing RE^{3+}

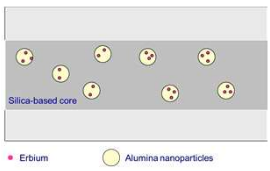

- O. Podrazky, I. Kasik, M. Pospisilova, and V. Matejec, "Use of alumina nanoparticles for preparation of erbium-doped fibers," in Proc. ***LEOS 2007*** *- IEEE Lasers and Electro-Optics Society Annual Meeting Conference Proceedings*, Orlando, Florida, USA, 21-25 Oct. 2007, pp. 246-247. https://doi.org/10.1109/leos.2007.4382369
- C. C. Baker, *et al.*, *Opt. Express* **25**, 13903-13915 (2017).
- M. Kamrádek, *et al.*, *IEEE Photonics J.* **11**, 7103610 (2019).

Pedestal refractive index profiles

Nanoparticle doping method (and other advanced methods) allow:
> 10 mol % of alumina (1 mol % ~ 2-2.3×10^{-3} r.i.u.)
> 1 mol % of Tm_2O_3 (1 mol % ~ 6.7×10^{-3} r.i.u.)
→ higher Δn than desired

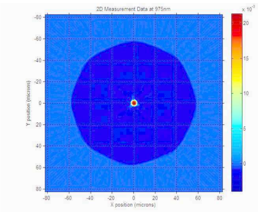

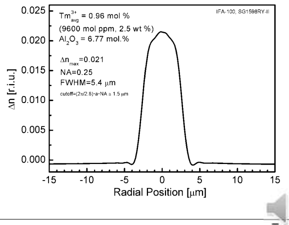

Drawing of optical fiber from preform

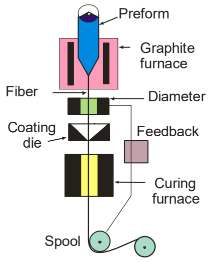

Diameter:

80-1000 μm

Graphite furnace temperature:

1800-2100°C

Pedestal refractive index profiles

Nanoparticle doping method (and other advanced methods) allow:
> 10 mol % of alumina (1 mol % ~ 2-2.3×10^{-3} r.i.u.)
> 1 mol % of Tm_2O_3 (1 mol % ~ 6.7×10^{-3} r.i.u.)
→ higher Δn than desired

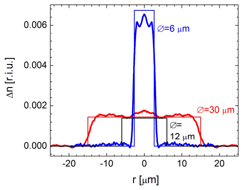

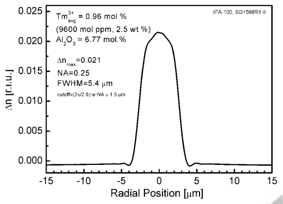

Optical Fiber Technology

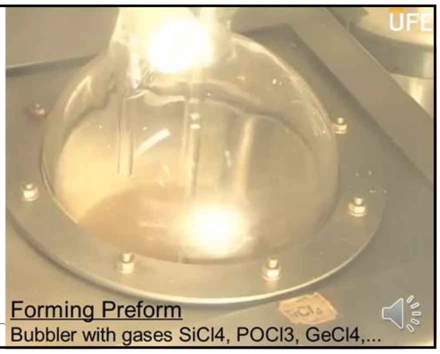

Pedestal refractive index profiles

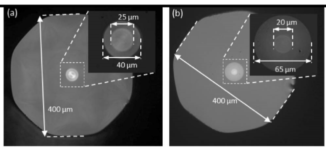

Fig. 1. a) End-face view of a 25P/400-TDF with a 25 μm core, 40 μm pedestal and a 400 μm flat-to-flat octagonal cladding. b) End-face view of a 20LP/400-TDF with a 20 μm core, 65 μm pedestal and a 400 μm flat-to-flat octagonal cladding.

N. Simakov, A. V. Hemming, A. Carter, K. Farley, A. Davidson, N. Carmody, M. Hughes, J. M. O. Daniel, L. Corena, D. Stepanov, and J. Haub, "Design and experimental demonstration of a large pedestal thulium-doped fibre," *Opt. Express* **23**(3), 3126-3133 (2015).

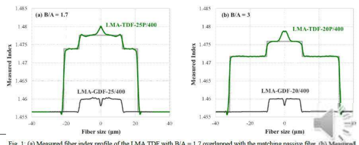

Fig. 1: (a) Measured fiber index profile of the LMA TDF with B/A = 1.7 overlapped with the matching passive fiber. (b) Measured index profile of the LMA TDF with B/A = 3 overlapped with the matching passive fiber.

C. Jollivet, K. Farley, M. Conroy, H. Dabhi, J. Edgecumbe, A. Carter, and K. Tankala, "Design optimization of Tm-doped large-mode area fibers for power scaling of 2 μm lasers and amplifiers," in Proc. SPIE **10083**, ***Photonics West***, San Francisco, USA, 2017, p. 100830I.

Shaping of optical fiber preforms by grinding or milling

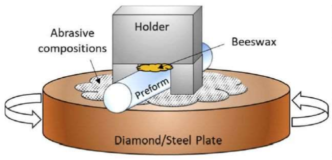

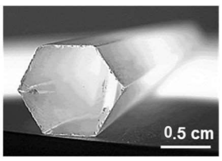

A. A. Jasim, O. Podrazký, P. Peterka, M. Kamrádek, I. Kašík, and P. Honzátko, "Impact of shaping optical fiber preforms based on grinding and a CO2 laser on the inner-cladding losses of shaped double-clad fibers," *Opt. Express* **28**, 13601-13615 (2020).

Thermal shaping of preforms

The outside interface of the pump-clad can be constructed from a rod-shaped preform by local melt-displacement using an open flame.

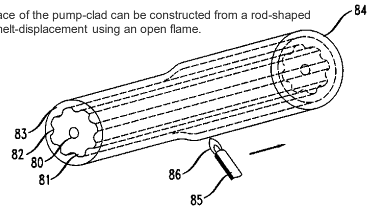

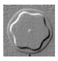

D. J. DiGiovanni, "Method of making a cladding pumped fiber structure," U. S. Patent 5 873 923, 23 Feb. 1999.

Shaping of optical fiber preforms by CO_2 laser

A. A. Jasim, O. Podrazký, P. Peterka, M. Kamrádek, I. Kašík, and P. Honzátko, "Impact of shaping optical fiber preforms based on grinding and a CO_2 laser on the inner-cladding losses of shaped double-clad fibers," *Opt. Express* **28**, 13601-13615 (2020).

P. C. Shardlow, R. Standish, J. Sahu, and W. A. Clarkson, "Cladding shaping of optical fibre preforms via CO_2 laser machining," in Proc. CLEO/Europe, Munich, 21 June 2015, p. CJ.P.29.

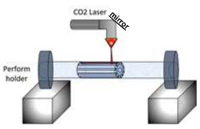

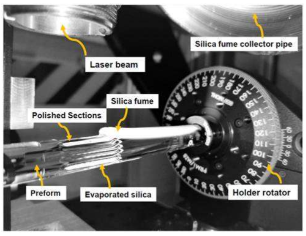

Ali A. Jasim

Pavel Honzátko

CO_2 polished preforms

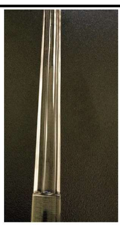

Sixfold shaped preform

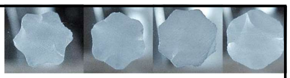

Shaped silica rods, cross sections

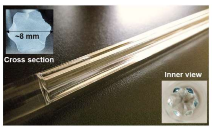

Features:

- Enables shaping preforms with concave and convex structures
- Short time of process (depends on laser power)
- Fully automated process

This technique profits from a high absorption of the silica glass at wavelengths around 10.6 µm

A. A. Jasim, *et al.*, *Opt. Express* **28**, 13601 (2020).

Drawn fibers

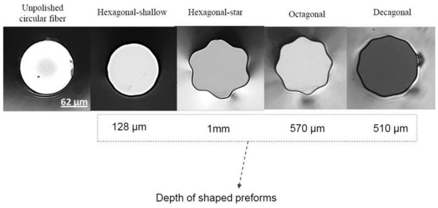

A. A. Jasim, *et al.*, *Opt. Express* **28**, 13601 (2020).

Main types of second claddings

Low-index acrylate coatings, typ. NA=0.46

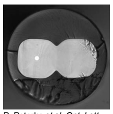

P. Peterka *et al*, *Opt. Lett.* **31**, 3240 (2006)

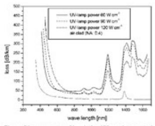

Figure 6 Loss spectra of low index UV-acrylate coated F300 fibers (DSM 1D3-63), the coating was cured with different UV lamp power density (The loss graph of the air clad fiber is pictured to reveal coating absorption effects.)

browning at less than 100 °C, High attenuation around 1.7-2 µm → cannot be used for tandem pumped Tm, or Ho fiber lasers

K. Schuster *et al*, "High NA fibers - A Comparison of Optical, Thermal and Mechanical Properties of Ultra Low Index Coated Fibers and Air Clad MOFs", 54th Int. Wired and Cable Symposium, 2005

Fluorine doped silica cladding, typ. NA=0.22

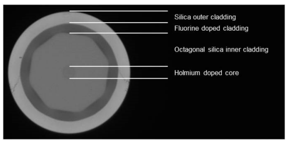

lower NA, but withstand high temperature

A. Hemming, S. Bennetts, N. Simakov, A. Davidson, J. Haub, and A. Carter, "High power operation of cladding pumped holmium-doped silica fibre lasers," *Opt. Express* **21**(4), 4560-4566 (2013).

Air-clad DC Fibers

NA determined by a propag. const. $\beta=k_0 n_{ef,slab}$ of the first mode excited in the capillary bridge:

$$NA = \sqrt{n_{silica}^2 - n_{ef,slab}^2}$$

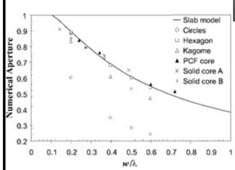

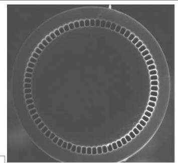

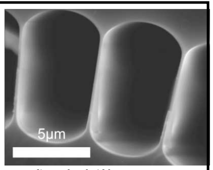

Inner cladding diameter 140 µm. 76 suspending webs of width 220 nm. Measured NA is represented with crosses ×

W. J. Wadsworth, R. M. Percival, G. Bouwmans, J. C. Knight, T. A. Birks, T. D. Hedley and P. S. J. Russell. Very high numerical aperture fibers. *IEEE Photonics Technol. Lett.* **16**, 843–845 (2004).

Agenda

I. Introduction 2
II. Fundamental principles, pump absorption 7
III. Limitations & LMA fibers 38
IV. Pump combiners 60
V. Technology 69
VI. Characterization 85
VII. Emerging technologies & Prospects 91

Absorption & emission

Cut-back method for **core** absorption (**cladding** abs. discussed before)

$$\frac{P_{out}}{P_{in}} = \exp(-\alpha L) = \exp(-\sigma_a \Gamma N_{tot} L)$$

$$Attenuation[dB] = -10\log\frac{P_{out}}{P_{in}} = 4.34\sigma_a \Gamma N_{tot} L$$

High concentration problems: long lengths, high power broadband sources, low resolution OSA, traditional cut-back method is not often suitable

Y. Feng, B. M. Zhang, J. Zhao, S. Zhu, J. H. V. Price, and J. Nilsson, "Absorption measurement errors in single-mode fibers resulting from re-emission of radiation," *IEEE J. Quantum Electron.* **53**, 6800611 (2017).

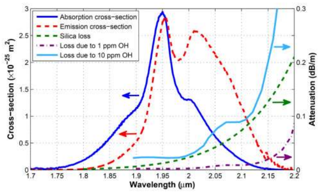

McCumber theory, indirect estimation of σ_e

$$\sigma_e(\nu) = \sigma_a(\nu)\exp\left(\frac{\varepsilon - h\nu}{kT}\right)$$

N. Simakov, A. Hemming, W. A. Clarkson, J. Haub, and A. Carter, "A cladding-pumped, tunable **holmium** doped fiber laser," *Opt. Express* **21**(23), 28415-28422 (2013).

Refractive index and concentration profiles

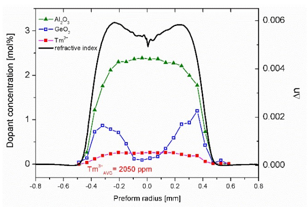

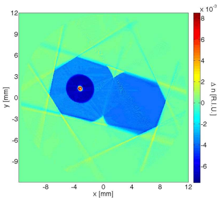

RIP - deflection function measurement, concentration - EMA (Electron Microprobe Analysis)

A. Novozamsky, J. Slanicka, and P. Peterka, "Tomography reconstruction of geometry and refractive index profile of highly asymmetric optical fiber preforms," SPIE **7746**, 77461O (2010).

Fluorescence lifetime

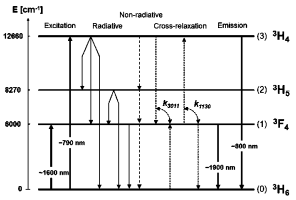

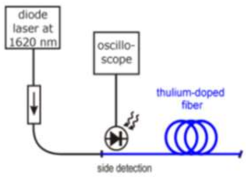

J. Cajzl, P. Peterka, M. Kowalczyk, J. Tarka, G. Sobon, J. Sotor, J. Aubrecht, P. Honzátko, and I. Kašík, "Thulium-doped silica fibers with enhanced fluorescence lifetime and their application in ultrafast fiber lasers," *Fibers* **6**(3), 66 (2018).

Absorption & emission

Cut-back method for **core** absorption (**cladding** abs. discussed before)

$$\frac{P_{out}}{P_{in}} = \exp(-\alpha L) = \exp(-\sigma_a \Gamma N_{tot} L)$$

$$Attenuation[dB] = -10\log\frac{P_{out}}{P_{in}} = 4.34\sigma_a \Gamma N_{tot} L$$

High concentration problems: long lengths, high power broadband sources, low resolution OSA, traditional cut-back method is not often suitable

Y. Feng, B. M. Zhang, J. Zhao, S. Zhu, J. H. V. Price, and J. Nilsson, "Absorption measurement errors in single-mode fibers resulting from re-emission of radiation," *IEEE J. Quantum Electron.* **53**, 6800611 (2017).

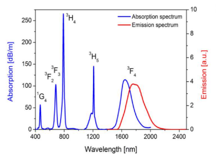

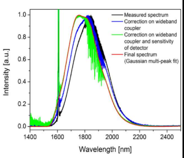

J. Cajzl, *et al.*, *Fibers* **6**, 66 (2018).

Emission spectral shape from fully inverted, very short (0.2 dB small-signal loss) fiber

Absolute value: gain in fully inverted fiber. **Estimation**: Judd-Ofelt theory & Fuchtbauer-Ladenburg formula

C.R. Giles *et al.*, *IEEE Photonics Technol. Lett.* **3**, 363 (1991).

Fluorescence lifetime

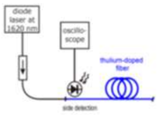

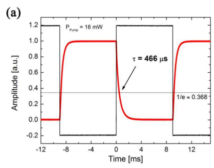

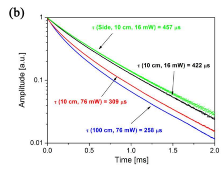

J. Cajzl, P. Peterka, M. Kowalczyk, J. Tarka, G. Sobon, J. Sotor, J. Aubrecht, P. Honzátko, and I. Kašík, "Thulium-doped silica fibers with enhanced fluorescence lifetime and their application in ultrafast fiber lasers," *Fibers* **6**(3), 66 (2018).

Agenda

I. Introduction 2
II. Fundamental principles, pump absorption 7
III. Limitations & LMA fibers 38
IV. Pump combiners 60
V. Technology 69
VI. Characterization 85
VII. Emerging technologies & Prospects 91

DC fiber for 10 kW single-mode diode-pumped fiber laser

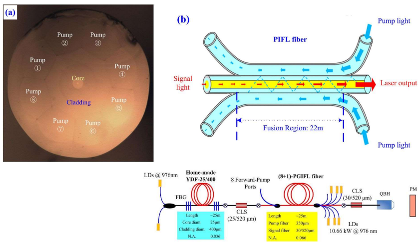

- avoid strong pump absorption,
- shortens the effective length of the signal
- distributes the thermal load along the fiber

→ mitigate SRS and TMI

8.72 kW @1080 nm, pump limited

H. Zhan, K. Peng, S. Liu, Y. Wang, Y. Li, X. Wang, L. Ni, S. Sun, J. Jiang, J. Yu, L. Jiang, J. Wang, F. Jing, and A. Lin, "**Pump-gain integrated functional laser** fiber **towards 10 kW**-level high-power applications," *Laser Phys. Lett.* **15**, 095107 (2018).

Nanostructured DC fibers

M. Franczyk, R. Stępień, A. Filipkowski, D. Pysz, and R. Buczyński, "Nanostructured core active fiber based on ytterbium doped phosphate glass," *IEEE J. Lightwave Technol.* **37**(23), 5885-5891 (2019).

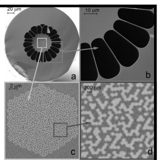

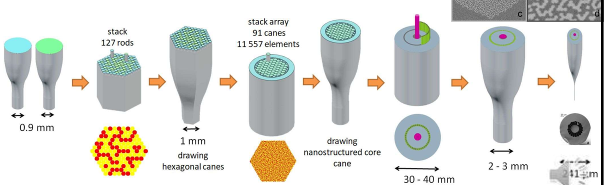

DC fibers for Mid IR lasers

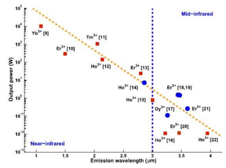

Fig. 1. Published laser power from rare-earth doped fiber laser as a function of operating wavelength [9]–[22]. The trend of reduced power as the wavelength increases (dashed orange line) is mostly a result of the energy difference between pump and laser photons. Recent development since 2012 [8] are marked with a blue circle. The Ho^{3+} based 3.9 μm laser required cryogenic cooling [22].

O. Henderson-Sapir, A. Malouf, N. Bawden, J. Munch, S. D. Jackson, and D. J. Ottaway, "Recent Advances in 3.5 μm Erbium-Doped Mid-Infrared Fiber Lasers," *IEEE J. Sel. Topics Quantum Electron.* **23**(3), (2017).

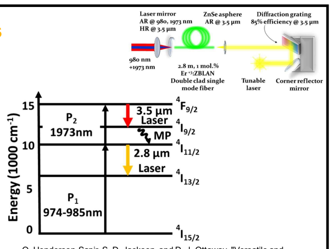

O. Henderson-Sapir, S. D. Jackson, and D. J. Ottaway, "Versatile and widely tunable mid-infrared erbium doped ZBLAN fiber laser," *Opt. Lett.* **41**, 1676-1679 (2016).

F. Maes, C. Stihler, L.-P. Pleau, V. Fortin, J. Limpert, M. Bernier, and R. Vallée, "3.42 μm lasing in heavily-erbium-doped fluoride fibers," *Opt. Express* **27**(3), 2170-2183 (2019).

Crystalline DC fibers

silica fibers drawbacks:
- low thermal conductivity (~1W/m/K),
- low dopant concentrations (<1%),
- and thermal effects (TMI, thermal lensing).
- SBS limits high power single frequency operation

YAG: ~100× lower SBS,
>10× higher thermal conductivity
high RE doping (~10 mol %)

(a) Various RE doped YAG and Sesquioxide feed rods used in this study. (b) A photograph image of 250μm diameter under a letter. (c) A looped fiber with a bend diameter of ~1 cm. (d) Microscope images of the endface of the 250 μm diameter crystal fibers. (e) Microscope images of the endface of the 35 μm diameter crystal fibers.

Source: Woohong Kim, Shyam Bayya, Brandon Shaw, Jason Myers, Syed N. Qadri, Rajesh Thapa, Dan Gibson, Collin Mcclain, Fred Kung, Joseph Kolis, Bradley Stadelman, and Jasbinder Sanghera, "Hydrothermally cladded crystalline fibers for laser applications [Invited]," *Opt. Mater. Express* **9**, 2716-2728 (2019)

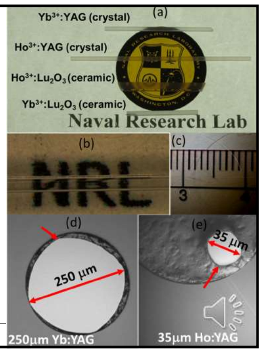

Advanced coatings

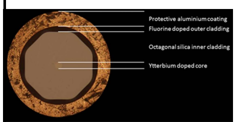

Cross-sectional view of the metal coated active fibre with all-glass inner cladding and ytterbium doped core. Fibre dimensions were 20/200/230 μm with numerical apertures of 0.075 and 0.23 for core, inner cladding and outer cladding respectively.

~40 °C lower temperture in the core in metal coated fiber

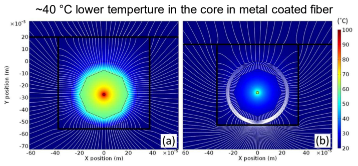

Thermal profiles of a) polymer and b) metal coated fibre lasers under a 100W/m thermal load with an interstitial material thermal conductivity of 1W/mK and 5μm offset from heatsink base.

J. M. O. Daniel, N. Simakov, A. Hemming, W. A. Clarkson, and J. Haub, "Metal clad active fibres for power scaling and thermal management at kW power levels," *Opt. Express* **24**(16), 18592-18606 (2016).

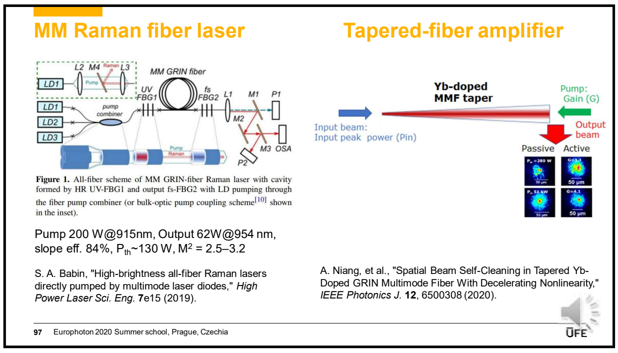
MM Raman fiber laser
Tapered-fiber amplifier
L2 M4 Raman L3
LD1 Pump
MM GRIN fiber
UV FBG1
fs FBG2
L1 M1 P1
LD1
pump combiner
LD2
LD3
M2
M3 OSA
P2
Pump
Raman
Figure 1. All-fiber scheme of MM GRIN-fiber Raman laser with cavity formed by HR UV-FBG1 and output fs-FBG2 with LD pumping through the fiber pump combiner (or bulk-optic pump coupling scheme[10] shown in the inset).
Pump 200 W@915nm, Output 62W@954 nm, slope eff. 84%, P_{th}~130 W, M^2 = 2.5–3.2
S. A. Babin, "High-brightness all-fiber Raman lasers directly pumped by multimode laser diodes," *High Power Laser Sci. Eng.* **7**e15 (2019).
Yb-doped MMF taper
Pump: Gain (G)
Input beam: Input peak power (Pin)
Output beam
Passive
Active
50 µm
50 µm
A. Niang, et al., "Spatial Beam Self-Cleaning in Tapered Yb-Doped GRIN Multimode Fiber With Decelerating Nonlinearity," *IEEE Photonics J.* **12**, 6500308 (2020).
97 Europhoton 2020 Summer school, Prague, Czechia
ÚFE


Team of Fiber Lasers and Nonlinear Optics